

ORIGINAL RESEARCH PAPER

# Effect of Shot Peening Parameters of AISI 420 on Stress and Roughness: An Analysis Using the Finite Element Method and the Response Surface Methodology

M. Hassanzadeh, S.E. Moussavi Torshizi\*

Faculty of Mechanical and Energy Engineering, Shahid Beheshti University, A.C., Tehran, Iran.

## Article info

### Article history:

Received 24 June 2020

Received in revised form

10 September 2020

Accepted 14 September 2020

### Keywords:

Shot peening

Finite element method

Response Surface Methodology (RSM)

Residual stresses

Roughness

## Abstract

This paper aimed to study the process of shot peening using the combination of the Finite Element Analysis (FEA) and the Response Surface Methodology (RSM). The shot velocity, shot diameter, coverage percentage and thickness are selected as process parameters. Residual compressive stresses and roughness are considered as response variables. Using FEA, shot peening is simulated and RSM is employed to determine the governing models between the response variables and the input parameters. The statistical analysis of the results reveals that: (1) the induced surface stress depends upon the coverage percentage and sample thickness, and it is independent of the shot velocity and shot diameter, (2) the maximum compression stress depends on the coverage percentage and shot diameter respectively, (3) the depth of maximum compressive stress depends on shot velocity and shot diameter respectively, (4) the depth of compressive stress is dependent on all four factors, (5) the roughness, Ra, is only dependent on the shot velocity. The results are in good agreement with the experimental data of the literature.

## 1. Introduction

Shot peening is frequently considered as an effective approach for enhancing the mechanical components behavior against fatigue [1-3]. One can attribute the advantageous effects of the process to the surface hardening and the residual stresses field [2, 3]. The results of shot peening are dependent on the mechanical features of the desired material and the conditions of the process (shot type, shot velocity, coverage, impact angle, etc.). Sometimes, when the parameters of shot peening are not chosen properly, one can see adverse effects on fatigue resistance [2, 3]. This issue demonstrates that the effect of shot peening on the performance of fatigue depends on process parameters selection. Therefore, it

is critical to estimate the shot peening parameters impacts on the fatigue behavior of the metal pieces and to select it optimally and appropriately.

Numerical, analytical, and experimental approaches can be used to estimate the shot peening effects. Hills et al. [4], Al-Obaid [5], and Al-Hassani [6] presented analytical approaches to estimate the shot peening residual stress. The use of analytic approaches is encountered some restrictions; therefore, a great deal empirical research has been carried out on the shot peening field. Obata and Sudo [7] and Dorr et al. [8] investigated the contribution of shot velocity and size to surface roughness and residual stress to the surface. Ahmed et al. [9] investigated the effect of different parameters of shot peening on the micro-hardness, resid-

\*Corresponding author: S.E. Moussavi Torshizi (Associate Professor)

E-mail address: e\_moussavi@sbu.ac.ir

<http://dx.doi.org/10.22084/jrstan.2020.22499.1157>

ISSN: 2588-2597

ual compressive stress, corrosion behavior, and wet-tability behavior of steel AISI 316L. Through a completely factorial design technique, Mahagaonkar et al. [10] investigated the effects of the exposure time, shot type, air pressure and nozzle distance and their interference impacts on steel micro-hardness. Nam et al. [11] examined the effects of pressure, nozzle distance, exposure time, and impact angle on micro-hardness and residual compressive stress of aluminum 2124-T851 using response surface methodology.

In comparison with the experimental test, one can use numerical simulation to reduce time and costs. A single-shot contact model was simulated by Hong et al. [12]. They investigated the contribution of the parameters including impact velocity, shot diameter, material properties and impact angle to the distribution of residual stresses at the desired surface. Meguid et al. [13] presented a symmetric model for a quarter of the shot in which the effects of single shot and two shots on the target surface were studied. In order to investigate the contribution of major parameters such as shot size and velocity on Almen intensity and residual stress, Guagliano [14] presented a finite element model with five-shot contact. Numerous shot impacts have been lately applied for the simulation of shot peening process to get more realistic results. Kim et al. [15], Cheng et al. [16] and Meguid et al. [17] developed some ideal models with regular distribution of the shots. However, for the completely randomized distribution of shots, closer to the real shot peening model in comparison with uniformly distributed models of shots, a number of models were developed by Ghasemi et al. [18], Miao et al. [19], and Mahmoudi et al. [20].

It has been observed that many studies were performed on the simulation of the shot peening process, but insufficient studies were done on the statistical model. In the literature, the statistical model was not used to interpret and understand the shot peening process. In addition, the relation between numerical and experimental was not investigated. Furthermore, the effect of the thickness of the shot-peened sample has not been investigated on responses so far.

This paper aimed to extract the statistical model to investigate the significance of the parameters of shot peening with respect to surface roughness and residual compressive stress. The design of experiments was performed with three levels to evaluate the effect and interaction between various parameters and its impact on the features of the shot peening surface. The most important phases of the presented approach can be summarized as follows:

- (i) Development and improvement of a finite element model through a randomized repeated procedure of the shot impact.
- (ii) DoE approach and numerical simulations.

- (iii) Extraction of the statistical model and their interpretation through statistical methods.

## 2. Finite Element Model

The finite element method was used to calculate the displacements, stresses and other quantities. The simulation of shot peening was done using the commercial code ABAQUS 2017. The explicit solver (explicit) was used to consider the dynamic effects of shot peening. In order to automatically generate a model with specific inputs (shot peening conditions, target material, boundary conditions, type of the shots and so on) the code was written based on the Python script. FEM analysis was developed using a damping coefficient [21] to reduce stress oscillations and to avoid uncontrolled oscillations after impact in the FEM model.

The material damping was introduced as being Eq. (1).

$$D = \alpha M + \beta K \quad (1)$$

where  $D$ ,  $M$  and  $K$  are the damping, mass and stiffness matrices, respectively. By using different values of  $\beta$ , the smoothness of the stresses on the surface of the body was compared with each other, and finally the value of  $2 \times 10^{-9}$ s was considered. For all sizes  $\beta$  was considered constant. Due to the range of dimensions, the effect of dimensions on  $\beta$  is negligible to eliminate fluctuations. To obtain reliable values of mass proportional damping  $\alpha$ , the following approach was adopted. The minimal modal frequency  $\omega_0$  could be estimated as in Eq. (2).

$$\omega_0 = \frac{1}{H} \sqrt{\frac{2E}{\rho}} \quad (2)$$

where  $E$  is the target Young's modulus,  $\rho$  is its density and  $H$  is the thickness of the target. The mass proportional damping was then determined as in Eq. (3).

$$\alpha = 2\omega_0\xi \quad (3)$$

where  $\xi$  is the corresponding modal damping parameter. In this study,  $\xi$  was selected 0.5 to decay the unwanted low-frequency oscillations [22].

Thermal and spring-back effects were neglected because of the negligible impact on the results. The proposed 3D model predicted residual compressive stress, plastic deformation, and surface integrity.

### 2.1. Boundary Condition and Geometry

In order to reduce the effect of the target edges and according to results of ref. [23], the target was modeled with dimensions of  $6D \times 6D \times h$ , where  $D$  is the diameter of the shot and  $h$  is the target thickness. The only

central area with dimensions of  $2D \times 2D$  in upper surface was encountered with multiple shots as seen in Fig. 1. The target was meshed by eight-node linear brick solid elements with reduced integration C3D8R. To improve the accuracy and efficiency of the results, a fine-mesh grid arrangement  $0.02\text{mm} \times 0.02\text{mm} \times 0.02\text{mm}$  for the shot peened area and a greater mesh size was considered for the rest of the body. General contact (Explicit) was used for the contact. All the target surfaces except the upper surface were fixed. The size of the model was considered large enough with respect to the size of the shot to eliminate the effects of the boundary condition. Without applying the constraint in the vertical direction, similar results would be achieved. The initial velocity applied to the shots perpendicular to the upper surface of the body ( $y$ -axis) and were fixed in the other directions.

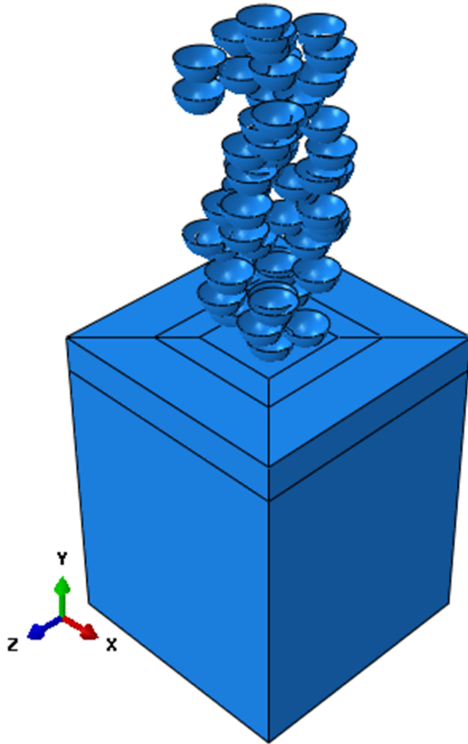


**Fig. 1.** A three-dimensional finite element model of shot peening.

## 2.2. Material Model

The target material was AISI 420 martensitic stainless steel and Johnson-Cook model was considered to simulate this material (Eq. (4)).

$$\sigma = (A + B(\varepsilon^p)^n) \left( 1 + C \log \left( \frac{\dot{\varepsilon}^p}{\dot{\varepsilon}_0} \right) \right) \left( 1 - \left( \frac{T - T_r}{T_m - T_r} \right)^m \right) \quad (4)$$

where  $A$ ,  $B$ ,  $C$ ,  $n$  and  $m$  are the constants of the material obtained by mechanical tests. The parameters  $\varepsilon^p$ ,  $\dot{\varepsilon}^p$ ,  $\dot{\varepsilon}_0$ ,  $T_r$ ,  $T_m$  and  $T$  are the equivalent plastic strain, the plastic strain rate, the reference strain rate, the room temperature, the melting temperature and reference temperature, respectively. Johnson Cook's parameters and other material parameters for AISI 420 were presented in Tables 1 and 2. The shots were considered analytically rigid.

## 2.3. Shot Stream Simulation

All of the mentioned shots were perpendicular to the surface. The following basic parameters were similarly assigned to the whole shots: velocity in  $V_y$  direction, diameter ( $D$ ), the friction between the shots and the target surface by the Columbian friction model (Eq. (5)):

$$F_f = \mu F_n \quad (5)$$

where  $F_n$  is the normal force,  $F_f$  is the friction force, and  $\mu$  is the friction coefficient. The friction coefficient for the contact between the shots and the target was chosen as 0.2, since the results of residual stress would not change much for a friction coefficient larger than 0.2 according to the literature [25, 26]. The number of shots is associated with the shot size, the coverage percentage, and the severity of the collision. The penalty formulation was used to formulate friction property in ABAQUS.

**Table 1**

Johnson-Cook parameters for the AISI 420 steel material [24].

A (MPa)	B (MPa)	C	n	m	$T_r$ (°C)	$T_m$ (°C)	$\dot{\varepsilon}_0$
450	738	0.02	0.338	0.8	27	1454	1

**Table 2**

Physical and mechanical properties for the AISI 420 steel material [24].

Density (g/cm <sup>3</sup> )	Poisson's ratio	Young's modulus (GPa)	Thermal conductivity (W/mK)	Specific heat (J/kg°C)	Thermal expansion (10 <sup>-6</sup> °C)
7.8	0.3	200	24.9	460	10.3

In case the shots hit the target successively, the time required for simulation is  $N\Delta t$ , where  $N$  is the quantity of shots and  $\Delta t$  is the time interval between the impacts; however, in case a number of shots simultaneously hit the target surface, the whole simulation time decreases. For this reason, several rows were assumed for the shots, each of which spaced from the surface proportional to the impact time. The origin of the coordinates was placed at the center of the target surface so that the  $y$ -axis was perpendicular to the surface. The shots position in  $x - z$  plane varied randomly from one row to another to generate a random impact condition. Therefore, the total time needed for simulation is only  $N_y\Delta t$  where  $N_y$  is the number of shots rows that is less than  $N$  in accordance with the number of shots per plane. The modeling phases were as following:

- (1) A local coordinate system was created at the center of the material surface, so that the  $y$ -axis remains perpendicular to the surface.
- (2) By using the random function, the center coordinates  $j$ -th shot ( $j \geq 1$ ) was generated in  $k$ -th row:

$$\begin{aligned} x_{kj} &= \text{random.uniform}(-d, d) \\ z_{kj} &= \text{random.uniform}(-d, d) \\ y_{kj} &= (k-1)V\Delta t + \frac{d}{2} \\ j &= 1, \dots, N_s, \quad k = 1, \dots, N_y \end{aligned} \quad (6)$$

where  $N_s$  is the number of shots for each row, and  $N_y$  is the number of rows of shots ( $N_y = N/N_s$ )  $\text{random.uniform}(-d, d)$  is a random number created in the range  $(-d, d)$  uniformly,  $\Delta t$  is the time interval between the successive shot hits, which is  $3.5 \times 10^{-6}$ s for our model, and  $d$  was the shot diameter.

- (3) The distance between the center of the  $i$ -th shot and the center of the  $j$ -th shot was determined through Eq. (7).

$$d_{i,j} = \sqrt{(x_j - x_i)^2 + (z_j - z_i)^2} \quad (7)$$

In case  $d_{i,j} < d$ , the shot  $j$  overlaps with the previous shot  $i$ , which is not possible physically. The shot  $j$  ought to be removed and return to step 2.

- (4) Go back to step (2) to generate the next shot center coordinates until the creation of the whole shots is finished.

#### 2.4. Shot Peening Coverage

The shot peening coverage is described as the ratio of the shot area to the total surface area. In statistical sense, the coverage of 100% is obtained only when the target shot peening is continued for an infinite time,

whilst this overlap does not affect the coverage. Generally, coverage of 98% is roughly considered as 100%, and the coverage of 200% is described as twice as long as required to reach 100% [1]. Apparently, the shot peening coverage has been generated on the basis of the dimple dimensions and the shot peening time. One can use the Avrami equation to assess the coverage [27]:

$$C = 100\% \times (1 - e^{-\pi r^2 R t}) \quad (8)$$

where  $C$  is the coverage,  $r$  indicates the mean dimple radius, and  $R$  is the number of shot hits in one second for the surface unit,  $t$  denotes the duration of shot peening time. Obviously  $R_t$  indicates the whole number of shots for the surface unit. The number of shots was obtained by the Avrami equation. First, the impact of a shot was modeled and its effect was selected as the value of the dimple. The number of rows was selected optionally so that it was logical and proportional with the size of the model. By dividing the number of shots to the number of rows, the number of shots per row was obtained.

### 3. Response Surface Methodology (RSM)

#### 3.1. Theory

The design of experiments includes a statistical approach for data gathering and prediction of the results on the basis of a limited number of inputs. This method is a systematic method for creating response surface as a function of input parameters. One can use RSM to analyze the experiment design results. When the whole independent variables are monitored and measured during the test, the response process is presented in:

$$Y = f(x_1, x_2, \dots, x_k) \quad (9)$$

In Eq. (9),  $k$  shows the number of independent variables. It is essential to find a logical function for the association between the response and independent variables. Therefore, the second-order polynomial function shown in Eq. (10) is usually utilized in response surface methodology (RSM) [11, 28]:

$$\begin{aligned} Y &= \beta_0 + \sum_{i=1}^k \beta_i x_i + \sum_{i=1}^k \beta_{ii} x_i^2 \\ &+ \sum_{i=1}^{k-1} \sum_{j=i+1}^k \beta_{ij} x_i x_j + \varepsilon \end{aligned} \quad (10)$$

In Eq. (10),  $\beta_0$  indicates the constant value,  $\beta_i$  shows the linear coefficients,  $\beta_{ii}$  denotes the second-order coefficients, indicates interaction coefficients, and  $\varepsilon$  is the model error. One can express Eq. (10) in the matrix form as Eq. (11):

$$Y = X \times B + \varepsilon \quad (11)$$



where  $\varepsilon$  is the vector of errors,  $Y$  represents the observation vector,  $B$  indicates the vector of the tuning parameters of the set, and  $X$  represents the matrix of the values of the design variables. Using the least squares regression, the regression coefficients are determined:

$$\hat{B} = (X^T X)^{-1} X^T Y \quad (12)$$

Thereafter, the fitted regression is determined by the following equation:

$$\hat{Y} = X \hat{B} \quad (13)$$

One can evaluate the goodness of fit using Eq. (14):

$$R^2 = 1 - \frac{\sum_i (Y_i - \hat{Y}_i)^2}{\sum_i (Y_i - \bar{Y}_i)^2} \quad (14)$$

where  $\hat{Y}_i$ ,  $\bar{Y}_i$ , and  $Y_i$  are the approximate value, the mean of the observed values, and the observed values, respectively.

### 3.2. Shot Peening Parameters and Responses Selection

In an experimental study, common parameters such as pressure, Almen intensity, shot diameter and so on are selected. However, in the present study because of numerical simulation of shot peening process, the parameters such as shot size, shot velocity, coverage, and target thickness were studied to link their effects to residual stress and roughness. Almen intensity is the criteria for measuring shot peening intensity. Almen intensity quantifies by a thin strip of SAE 1070 steel named Almen strip with dimensions of 76mm×19mm and three thicknesses. The thicknesses are 0.79mm, 1.29mm and 2.39mm for type *N*, *A* and *C* respectively. Almen strips are fixed by means of four bolts and shot peening operation is performed with the same shot peening parameters and different exposure time. When the peened strip is released, it will curve. The arc heights of the curve are measured under different exposure time. The Almen intensity is defined as the arc height at saturation which is the point, on the curve of peening time versus arc height, beyond which the arc height increases by less than 10% when the exposure time doubles. According to the Fig. 2 [29] it can be proposed that Almen intensity in the finite intervals is linear in relation to velocity.

The residual stresses included the residual stresses of the target surface ( $\sigma_{\text{surf}}^{\text{RS}}$ ) and the maximum induced residual stresses ( $\sigma_{\text{max}}^{\text{RS}}$ ). In addition, the depths of the maximum residual stress ( $\delta_{\text{max}}^{\text{RS}}$ ) and the compressive stress depth ( $\delta_c^{\text{RS}}$ ) were also considered in this study. For estimating the residual stress distribution, the av-

erage residual stress was calculated at each depth [30]:

$$\bar{\sigma}_{xx} = \frac{1}{N} \sum_{i=1}^N \sigma_{xx}(i) \quad (15)$$

where  $\bar{\sigma}_{xx}$  is the averaged value of stress  $\sigma_{xx}$ , and  $N$  is the number of the stress nodal values at that depth.

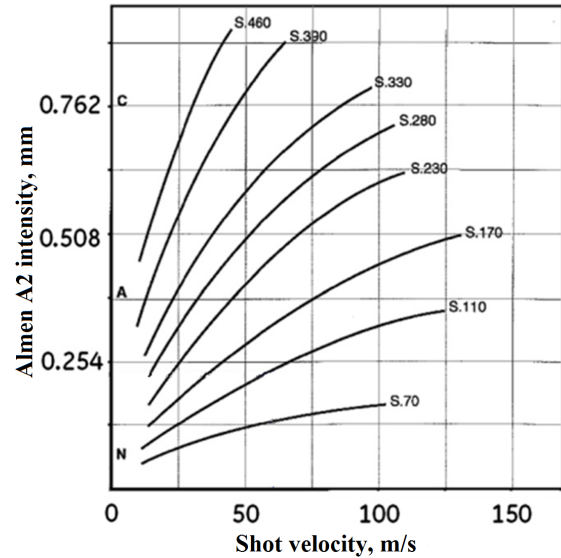


**Fig. 2.** Almen intensity vs. shot velocity for different shot sizes [29].

Surface treatment of shot peening is usually done to increase the strength of mechanical components of the metal. However, in many cases, there is the possibility of failure or alteration of the shot peened surface by surface defects such as micro-cracks and surface roughness defects [2, 3], which can significantly reduce the fatigue strength [31, 32]. Roughness defects are considered as a sequence of cavities due to shot peening.

Roughness includes the arithmetical mean deviation of the profile  $R_a$  and the mean height of the five dominant peaks and the five deep valleys  $R_c$ . The obtained data after Gaussian filtering steps represent the surface irregularity without the presence of the wave component. The displacement of the surface target in the mid line was selected as data. Fig. 3 shows an example of surface displacements after shot peening. The developed MATLAB routine provided the possibility of determining the parameters  $R_a$ ,  $R_c$  according to their standard definitions presented.

Each factor was tested at three different levels, highest (1), medium (0) and lowest (−1). Their related levels are shown in real and coded values in Table 3.

**Table 3**  
Input factors and their levels.

Parameter	Notation	Level		
		−1	0	+1
Shot size (mm)	d	0.5842	0.7112	0.8382
Shot velocity (m/s)	V	70	90	110
Peening coverage (%)	C	100	150	200
Plate thickness (mm)	h	3	4.5	6

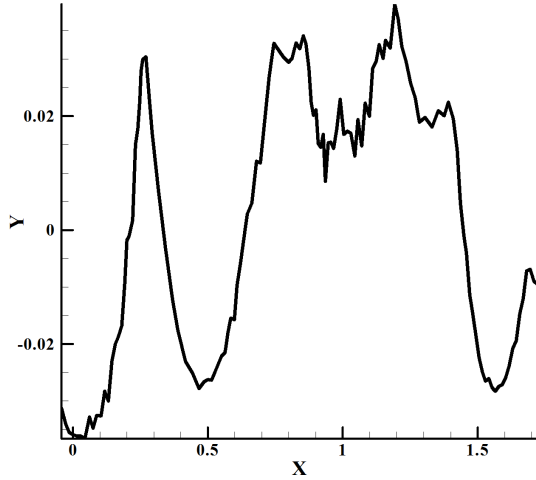


Fig. 3. Surface displacements after shot peening.

## 4. Results

The results of FEM simulation for various parameters according to the Box-Behnken design are shown in Table 4. The statistical analysis of results is done with Design Expert 11 software. Analysis of variance (ANOVA) uses  $P$ -value in order to check the signifi-

cance of the model and the effects of the independent variables on the responses. The  $P$ -value of less than 0.05 indicates a significant result [33]. If the term shows a  $P$ -value higher than 0.05, it means that the term in the model can be ignored.

### 4.1. The Mathematical Model of the Surface Stress

Stress at the top of the body ( $h = 0$ ) is the surface stress. Using the ordinary least squares, the appropriate equation for surface stress ( $\sigma_{\text{surf}}^{\text{RS}}$ ) with a polynomial degree of two is as follows:

$$\begin{aligned} \sigma_{\text{surf}}^{\text{RS}} = & 361.64 - 9.52V - 1168.20d - 6.90C + 125.83h \\ & + 0.081145V^2 + 355.25d^2 + 0.0043545C^2 - 10.85h^2 \\ & - 2.22Vd + 0.0092VC - 0.88525Vh + 3.79dC \\ & + 44.10dh + 0.2592Ch \end{aligned} \quad (16)$$

$$(R^2 = 0.8272 \text{ and Adjusted } R^2 = 0.5854)$$

Eq. (16) is more suitable for predicting results and is not suitable for determining important response parameters. It can use statistics and  $P$ -value to determine important parameters. The recommended model is a linear model for surface stress ( $\sigma_{\text{surf}}^{\text{RS}}$ ).

Table 4

The final matrix of the design of experiments and the results of the shot peening simulation for various inputs.

RUN	V (m/s)	d (mm)	C (%)	h (mm)	$\sigma_{\text{surf}}^{\text{RS}}$ (MPa)	$\sigma_{\text{max}}^{\text{RS}}$ (MPa)	$\delta_{\text{max}}^{\text{RS}}$ (mm)	$\delta_{\text{c}}^{\text{RS}}$ (mm)	Rc ( $\mu\text{m}$ )	Ra ( $\mu\text{m}$ )
1	110	0.7112	150	3	-737.0039	-1026.2839	0.1021	0.7718	11.4392	3.5075
2	90	0.5842	150	6	-715.3882	-988.7391	0.0721	0.5646	14.2873	3.6231
3	70	0.7112	150	6	-656.2845	-921.8067	0.0781	0.5826	11.9180	2.9833
4	70	0.5842	150	4.5	-751.2234	-992.5166	0.0676	0.4795	11.3565	3.4356
5	90	0.8382	200	4.5	-736.2363	-1094.0902	0.0991	0.8378	10.5295	4.1180
6	70	0.7112	100	4.5	-651.9672	-877.2058	0.0721	0.5586	11.6337	3.6414
7	90	0.7112	100	3	-711.8292	-971.2497	0.0781	0.6607	10.4972	3.3669
8	110	0.7112	100	4.5	-623.7722	-922.1007	0.1081	0.7613	15.1102	4.1356
9	90	0.5842	100	4.5	-644.9260	-909.4089	0.0766	0.5270	12.7927	3.2410
10	90	0.8382	150	3	-781.2282	-1057.9755	0.0841	0.7958	11.0446	3.6453
11	90	0.8382	150	6	-718.1584	-1035.4722	0.0961	0.8228	8.7978	2.8108
12	110	0.7112	150	6	-725.4332	-1042.3805	0.0901	0.8108	15.5082	3.9135
13	110	0.7112	200	4.5	-685.3791	-1060.1887	0.0991	0.8468	12.8203	3.9938
14	110	0.8382	150	4.5	-694.3964	-1004.2666	0.0766	0.9820	10.9870	3.6347
15	110	0.5842	150	4.5	-661.4981	-999.0297	0.0901	0.6532	11.3024	3.6695
16	70	0.8382	150	4.5	-761.6092	-1012.6668	0.0766	0.6802	10.1129	2.8386
17	90	0.7112	150	4.5	-735.9481	-1011.8378	0.0811	0.6982	12.8038	3.3431
18	90	0.7112	200	3	-883.7832	-1190.5149	0.0841	0.7177	11.2354	3.2967
19	90	0.7112	100	6	-692.8838	-955.4292	0.0781	0.6547	10.3430	2.9266
20	90	0.5842	200	4.5	-752.6129	-1036.9222	0.0721	0.5631	11.0186	3.3099
21	70	0.7112	200	4.5	-750.4079	-1030.2889	0.0721	0.5901	9.6687	3.3144
22	70	0.7112	150	3	-774.0852	-1005.7000	0.0721	0.5556	7.7528	2.6836
23	90	0.8382	100	4.5	-724.7551	-975.4200	0.0856	0.7748	14.1629	3.4474
24	90	0.5842	150	3	-744.8544	-981.5827	0.0721	0.5526	12.0294	3.3168
25	90	0.7112	200	6	-787.0832	-1068.1596	0.0781	0.7628	13.5839	3.5489

The effects of shot peening parameters are shown in Table 5 for  $\sigma_{\text{surf}}^{\text{RS}}$ . In the Table 5, “Model” means a mathematical model of the desired response. Other parameters show the effect of a particular parameter with respect to the response. By examining the  $P$ -value for different terms, one can conclude that the effective parameters are  $C$  and  $h$ , respectively.  $V$  and  $d$  have less effect than other parameters. The obtained model for  $\sigma_{\text{surf}}^{\text{RS}}$  is determined in:

$$\sigma_{\text{surf}}^{\text{RS}} = -672.15 - 0.09089C + 18.7529h \quad (17)$$

It can be seen from the Eq. (17) that in addition to the coverage percentage, the sample thickness is also effective on the value of  $\sigma_{\text{surf}}^{\text{RS}}$ . The effect of thickness is to reduce compressive stress. Fig. 4 shows 3D surface plot of  $\sigma_{\text{surf}}^{\text{RS}}$  versus the input parameters. It shows that the parameter  $C$  has the greatest impact.

#### 4.2. The Mathematical Model of the Maximum Compressive Stress

Similarly, for other responses, suitable models can be obtained by software. The obtained equation with a

polynomial degree of two for maximum compressive stress ( $\sigma_{\text{max}}^{\text{RS}}$ ) is as follows:

$$\begin{aligned} \sigma_{\text{max}}^{\text{RS}} = & -16.32 - 10.34V - 674.39d - 3.77C + 78.74h \\ & + 0.064390V^2 + 96.053d^2 + 0.00047528C^2 \\ & - 8.045h^2 + 1.47Vd + 0.0037488VC - 0.83325Vh \\ & + 0.34816dC + 38.92dh + 0.35512Ch \end{aligned} \quad (18)$$

( $R^2 = 0.8925$  and Adjusted  $R^2 = 0.7420$ ) However, the mathematical relation of appropriate statistical model for this response is linear and ANOVA analysis is presented in Table 6. The effective parameters are  $C$  and  $d$  respectively.  $V$  and  $h$  have less effect than  $C$  and  $d$ . The obtained model is:

$$\sigma_{\text{max}}^{\text{RS}} = -662.72 - 1.4489C - 178.276d \quad (19)$$

The effect of  $C$  and  $d$  are to increase compressive stress. Fig. 5 shows 3D surface plot of  $\sigma_{\text{max}}^{\text{RS}}$  versus the input parameters. It can be seen that the parameter  $C$  has the greatest impact.

**Table 5**

The results of ANOVA analysis of surface residual stresses ( $\sigma_{\text{surf}}^{\text{RS}}$ ) in the simulation of the shot peening process to determine the effect of various parameters.

Source	Sum of square	df	Mean square	$F$ -value	$P$ -value	
Model	40017.95	4	10004.49	5.99	0.0025	Significant
$V$	3963.76	1	3963.76	2.37	0.1392	Insignificant
$d$	1773.42	1	1773.42	1.06	0.3152	Insignificant
$C$	24785.61	1	24785.61	14.83	0.0010	Significant
$h$	9495.16	1	9495.16	5.68	0.0272	Significant
Residual	33417.73	20	1670.89			
Cor total	73435.68	24				

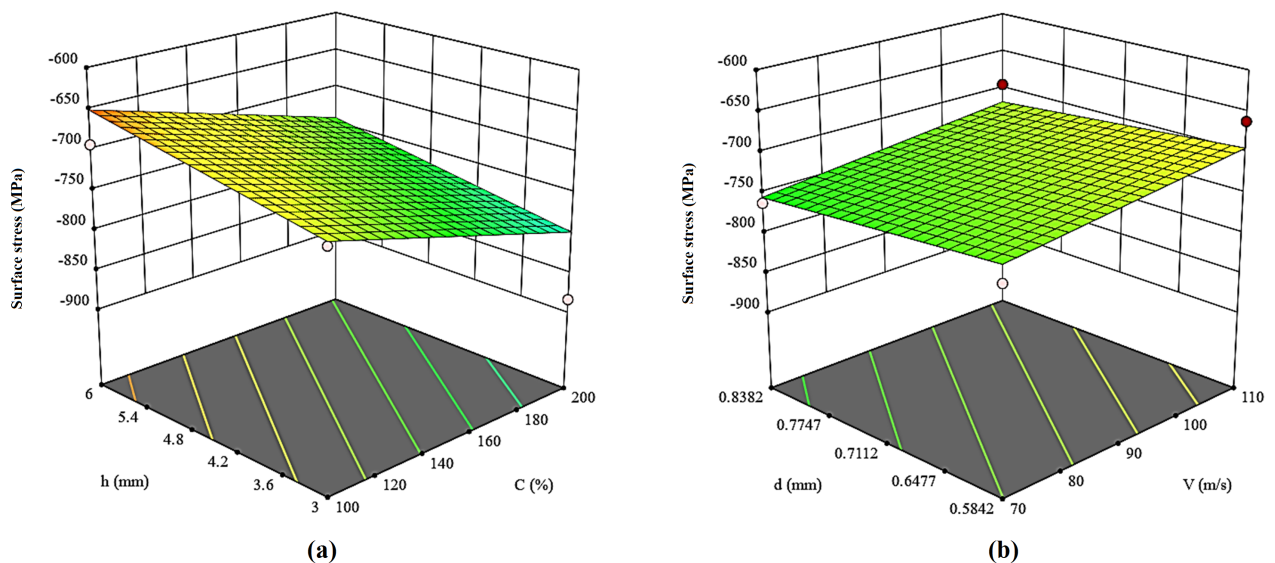


**Fig. 4.** 3D surface plot of surface stress versus a) Coverage and target thickness b) Shot velocity and shot diameter.

**Table 6**

The results of ANOVA analysis of the maximum compressive stress ( $\sigma_{\max}^{\text{RS}}$ ) in the simulation the shot peening process to determine the effects of various parameters.

Source	Sum of square	df	Mean square	F-value	P-value	
Model	77032.69	4	19258.17	15.81	< 0.0001	Significant
V	3818.66	1	3818.66	3.14	0.0918	Insignificant
d	6151.38	1	6151.38	5.05	0.0361	Insignificant
C	62980.80	1	62980.80	51.71	< 0.0001	Significant
h	4081.86	1	4081.86	3.35	0.0821	Insignificant
Residual	24357.96	20	1217.90			
Cor total	1.014E+05	24				

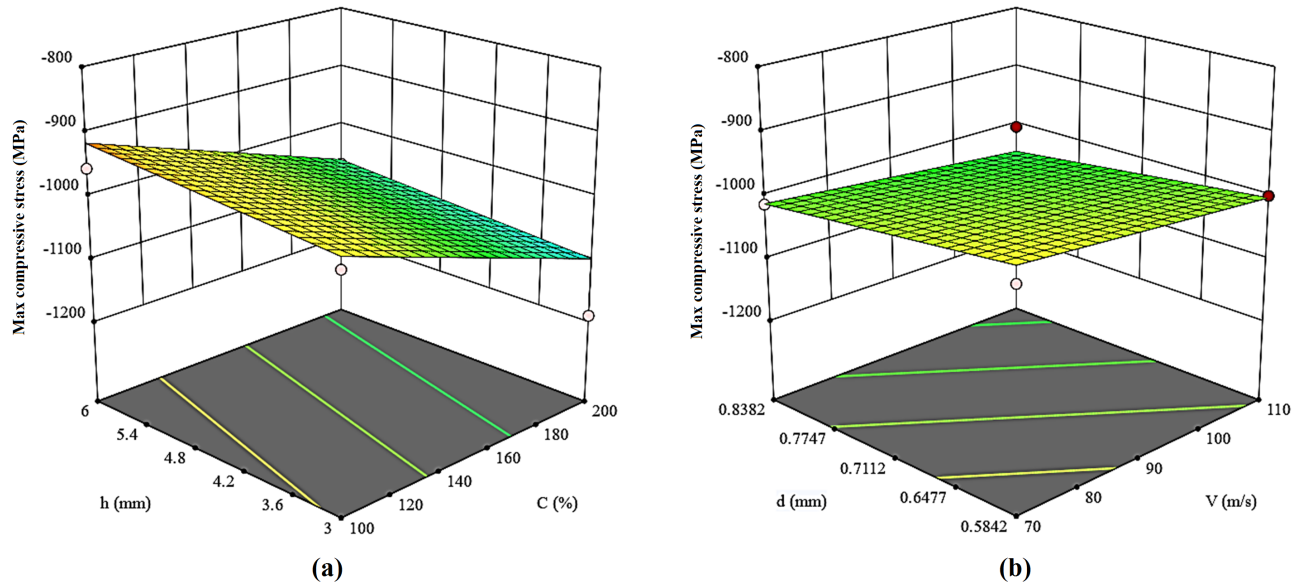


**Fig. 5.** 3D surface plot of maximum compressive stress versus a) Coverage and target thickness b) Shot velocity and shot diameter.

#### 4.3. The Mathematical Model of the Depth of the Maximum Compressive Stress

The equation with a polynomial degree of two for the depth of the maximum compressive stress ( $\delta_{\max}^{\text{RS}}$ ) is as follows:

$$\begin{aligned} \delta_{\max}^{\text{RS}} = & -0.11102 + 0.0019957V + 0.24306d \\ & - 0.00047948C + 0.0050551h + 6.26e \\ & - 06V^2 - 0.12412d^2 + 9.26e - 07C^2 \\ & + 2.78e - 05h^2 - 0.0022168Vd - 2.25e \\ & - 06VC - 0.00015015Vh + 0.00070937dC \\ & + 0.015764dh - 2.002e - 05Ch \end{aligned} \quad (20)$$

( $R^2 = 0.7436$  and Adjusted  $R^2 = 0.3846$ )

The appropriate statistical model for the depth of the maximum compressive stress ( $\delta_{\max}^{\text{RS}}$ ) is linear. The corresponding ANOVA analysis is presented in Table 7. It can be seen that the effective parameters are V and d. The thickness h has no effect on  $\delta_{\max}^{\text{RS}}$ . The resulting model is expressed as Eq. (21):

$$\delta_{\max}^{\text{RS}} = 0.003071 + 0.000532V + 0.04434d \quad (21)$$

Fig. 6 shows 3D surface plot of  $\delta_{\max}^{\text{RS}}$  versus the input parameters. It shows that the parameter V and d have the greatest impact.

#### 4.4. The Mathematical Model of the Compressive Stress Depth

The relation with a polynomial degree of two for the compressive stress depth ( $\delta_c^{\text{RS}}$ ) is as follows:

$$\begin{aligned} \delta_c^{\text{RS}} = & 0.25416381676828 - 0.0044239V \\ & + 0.31642d - 0.0015075C - 0.019184h - 7.088e \\ & - 06V^2 - 0.47834d^2 - 1.99e - 06C^2 - 0.0023729h^2 \\ & + 0.012612Vd + 1.35e - 05VC \\ & + 0.0001001Vh + 0.0010641dC \\ & + 0.019705dh + 0.00017017Ch \end{aligned} \quad (22)$$

( $R^2 = 0.9929$  and Adjusted  $R^2 = 0.9831$ )

The suitable statistical model for the compressive stress depth ( $\delta_c^{\text{RS}}$ ) is 2FI and the corresponding ANOVA is presented in Table 8. It is seen that the effective linear parameters are respectively d, V, C, h

and the nonlinear effective parameter is  $V \times d$ , respectively, and the resulting model is:

$$\delta_c^{RS} = 0.12183 - 0.003222V - 0.1157d + 0.00636C + 0.00801h + 0.01261Vd \quad (23)$$

Unlike  $\delta_{\max}^{RS}$ ,  $\delta_c^{RS}$  depends on  $h$ . The Eq. (23) shows that the  $\delta_c^{RS}$  has a complex relationship with different parameters. Fig. 7 shows 3D surface plot of  $\delta_c^{RS}$  versus the input parameters. It shows that the parameter  $d$  and  $V$  have the greatest impact.

**Table 7**

The results of ANOVA analysis of maximum compressive stress depth in the simulation the shot peening process to determine the effects of various parameters.

Source	Sum of square	df	Mean square	<i>F</i> -value	<i>P</i> -value	
Model	0.0017	4	0.0004	7.10	0.0010	Significant
<i>V</i>	0.0014	1	0.0014	22.15	0.0001	Insignificant
<i>d</i>	0.0004	1	0.0004	6.21	0.0216	Insignificant
<i>C</i>	3.006E-06	1	3.006E-06	0.0490	0.8270	Significant
<i>h</i>	2.168E-19	1	2.168E-19	3.538E-15	1.0000	Insignificant
Residual	0.0012	20	0.0001			
Cor total	0.0030	24				

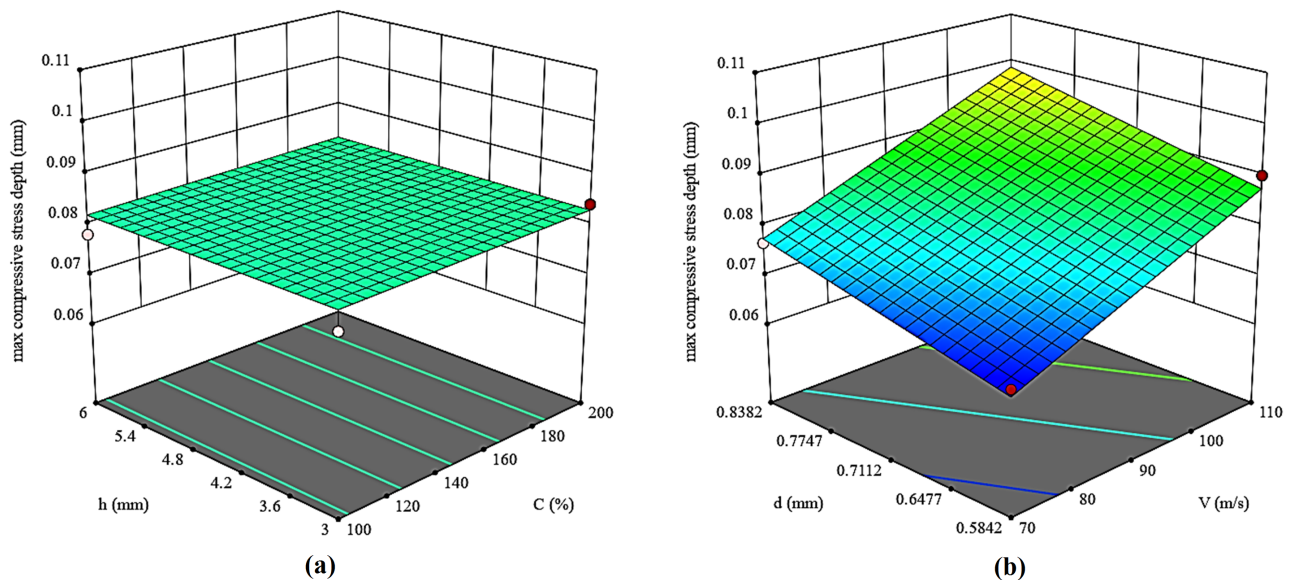


**Fig. 6.** 3D surface plot of maximum compressive stress versus a) Coverage and target thickness b) Shot velocity and shot diameter.

**Table 8**

The results of ANOVA analysis of compressive stress depth ( $\delta_c^{RS}$ ) in the simulation the shot peening process to determine the effects of various parameters.

Source	Sum of square	df	Mean square	<i>F</i> -value	<i>P</i> -value	
Model	0.3793	10	0.0379	183.35	< 0.0001	Significant
<i>V</i>	0.1586	1	0.1586	766.44	< 0.0001	Significant
<i>d</i>	0.2011	1	0.2011	972.22	< 0.0001	Significant
<i>C</i>	0.0121	1	0.0121	58.59	< 0.0001	Significant
<i>h</i>	0.0017	1	0.0017	8.37	0.0118	Significant
<i>Vd</i>	0.0041	1	0.0041	19.84	0.0005	Significant
<i>VC</i>	0.0007	1	0.0007	3.53	0.0812	Insignificant
<i>Vh</i>	0.0000	1	0.0000	0.1744	0.6826	Insignificant
<i>dC</i>	0.0002	1	0.0002	0.8827	0.3634	Insignificant
<i>dh</i>	0.0001	1	0.0001	0.2725	0.6099	Insignificant
<i>Ch</i>	0.0007	1	0.0007	3.15	0.0977	Insignificant
Residual	0.0029	14	0.0002			
Cor total	0.3822	24				



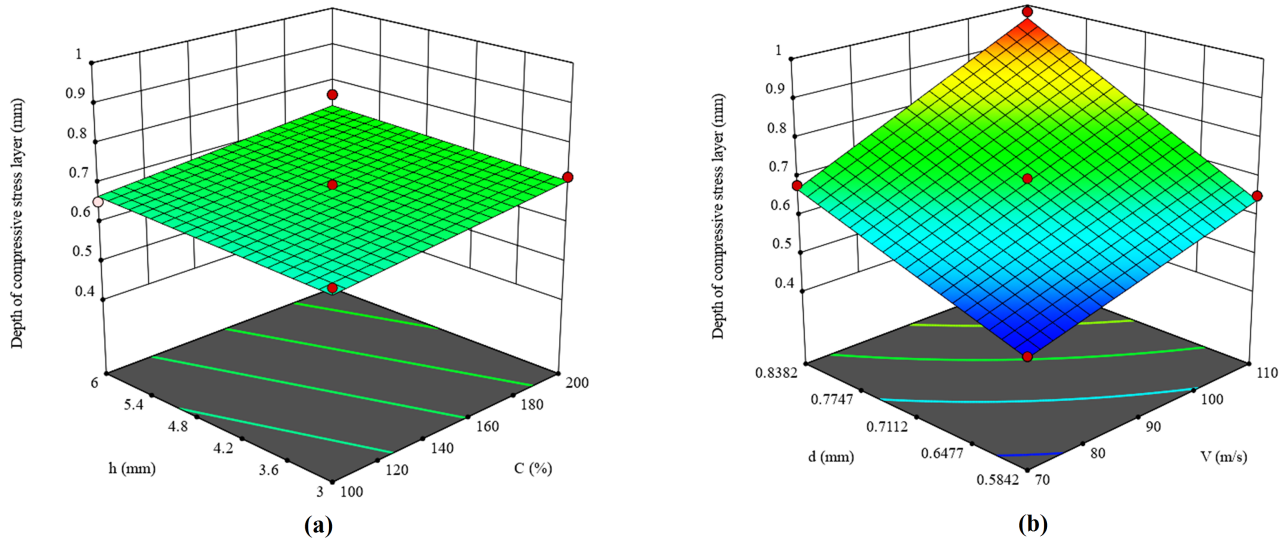


**Fig. 7.** 3D surface plot of depth of compressive stress layer versus a) Coverage and target thickness b) Shot velocity and shot diameter.

#### 4.5. The Mathematical Model of the Roughness Ra

The relation with a polynomial degree of two for roughness Ra is as follows:

$$\begin{aligned} Ra = & 9.1314083333337 - 0.085065V - 4.63d \\ & - 0.052539C + 1.2h + 0.00028483V^2 + 1.94d^2 \\ & + 7.5e - 05C^2 - 0.067613h^2 + 0.055335Vd \\ & + 4.63e - 05VC + 0.00088583Vh + 0.023689dC \\ & - 1.5dh + 0.0023083Ch \end{aligned} \quad (24)$$

( $R^2 = 0.6933$  and Adjusted  $R^2 = 0.2639$ )

The recommended statistical model is a linear model for roughness Ra. In Table 9 the effects of shot peening parameters are observed for Ra. By examining  $P$ -value for different terms, it is concluded that the effective parameter is  $V$ , and other parameters have a small effect on Ra.  $h$  and  $d$  have less effect than other parameters. The model obtained for Ra is expressed as:

$$Ra = 1.9457 + 0.01649V \quad (25)$$

Fig. 8 shows 3D surface plot of roughness Ra versus the input parameters. Fig. 8 shows that the parameter  $V$  has the greatest impact.

#### 4.6. The Mathematical Model of the Roughness Rc

Similarly, the relation with a polynomial degree of two for roughness Rc is as follows:

$$\begin{aligned} Rc = & -54.23 + 0.069416V + 121.96d - 0.082834C \\ & + 11.26h - 0.00097553V^2 - 103.89d^2 \\ & - 0.00011185C^2 - 0.29159h^2 + 0.48847Vd \\ & + 0.00010358VC - 0.037073Vh + 0.14212dC \\ & - 8.28dh + 0.0031807Ch \end{aligned} \quad (26)$$

( $R^2 = 0.6837$  and Adjusted  $R^2 = 0.2409$ ) ANOVA analysis can be performed for Rc roughness. The selected model for Rc is a linear model and the corresponding ANOVA is given in Table 10. It is again seen that  $V$  is an effective parameter and the resulting model is expressed as Eq. (27):

$$Rc = 7.035 + 0.08993V \quad (27)$$

**Table 9**

The results of the ANOVA analysis of roughness Ra in the simulation the shot peening process to determine the effects of various parameters.

Source	Sum of square	df	Mean square	F-value	P-value	
Model	1.36	4	0.3406	3.02	0.0424	Significant
$V$	1.31	1	1.31	11.57	0.0028	Insignificant
$d$	0.0009	1	0.0009	0.0075	0.9316	Insignificant
$C$	0.0564	1	0.0564	0.4999	0.4877	Significant
$h$	9.363E-06	1	9.363E-06	0.0001	0.9928	Insignificant
Residual	2.26	20	0.1129			
Cor total	3.62	24				

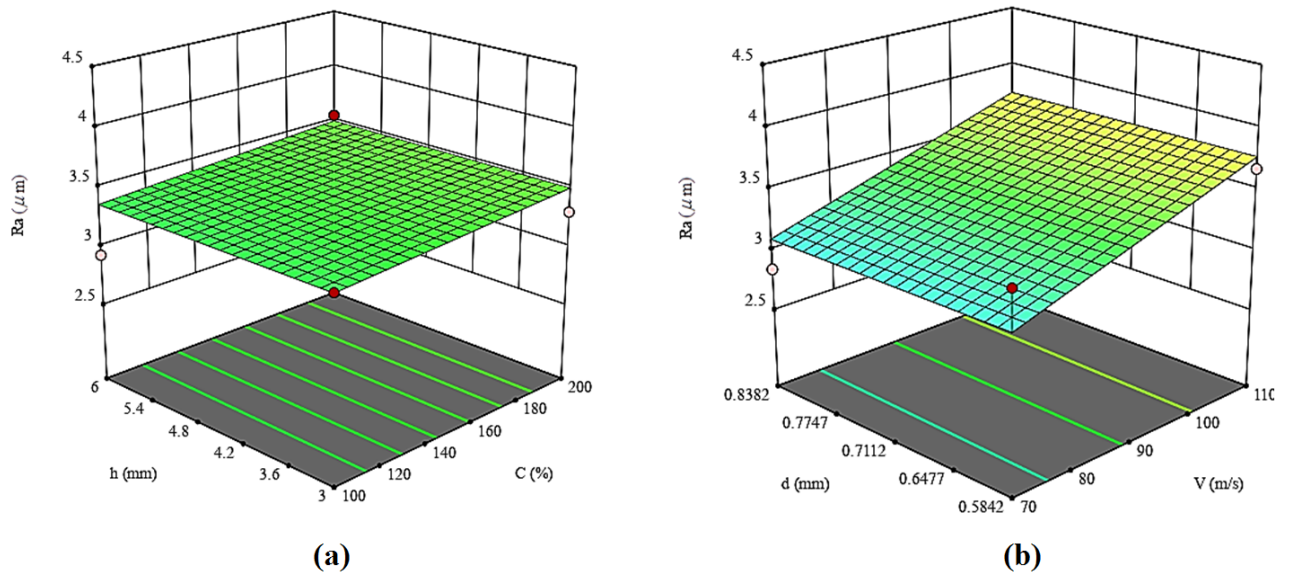


**Fig. 8.** 3D surface plot of roughness  $R_a$  versus a) Coverage and target thickness b) Shot velocity and shot diameter.

**Table 10**

The results of ANOVA analysis of roughness  $R_c$  in simulation of shot peening process to determine the effects of various parameters.

Source	Sum of square	df	Mean square	$F$ -value	$P$ -value	
Model	42.18	4	10.54	2.89	0.0485	Significant
$V$	38.82	1	38.82	10.66	0.0039	Significant
$d$	0.9672	1	0.9672	0.2655	0.6120	Insignificant
$C$	2.08	1	2.08	0.5706	0.4588	Insignificant
$h$	0.3088	1	0.3088	0.0848	0.7739	Insignificant
Residual	72.85	20	3.64			
Cor total	115.03	24				

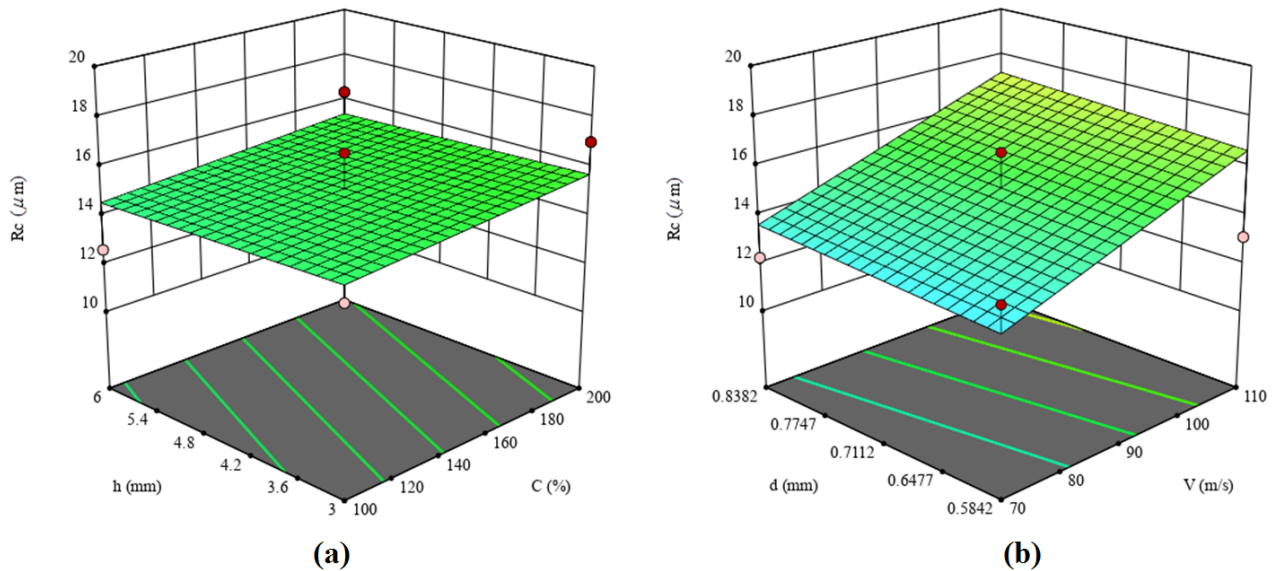


**Fig. 9.** 3D surface plot of roughness  $R_c$  versus a) Coverage and target thickness b) Shot velocity and shot diameter.

Fig. 9 shows 3D surface plot of roughness  $R_c$  versus the input parameters. It can be seen that the parameter  $V$  has the greatest impact.

## 5. Validation and Discussion

In this section, the models obtained from the results section were validated and compared with the experimental data. The operating conditions were as:



(i) Shot S170, (ii) Almen Intensity 14A, (equivalent to velocity 67.7m/s), (iii) Coverage 100%, (iv) Impact angles 90 degree, (v) Thickness 1.5mm.

The sample dimensions are shown in the Fig. 10. The coefficient of friction between the shots and the surface during the contact was 0.2.

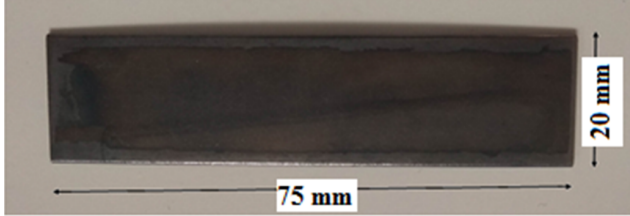


**Fig. 10.** Dimension of test specimens.

Fig. 11 shows the comparison between the XRD of experimental results and the residual compressive stress profile obtained numerically. XRD residual stress analysis and the electrolytic layer removal technique were used to obtain residual stress depth profiles. Stress relaxation due to layer removal was not taken into account, since the affected region was small and no significant relaxation effects could be expected. Residual stresses were calculated for the plain stress condition. A satisfactory correspondence was observed between the calculated results and experimental values. Fig. 12 shows the contour of the stress S11.

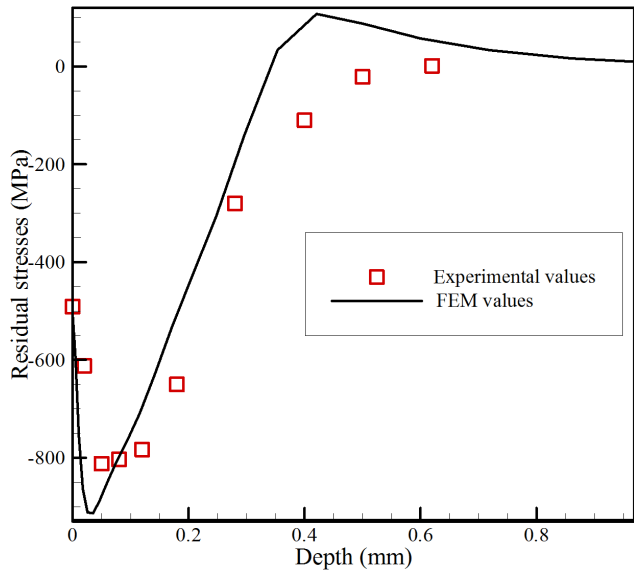


**Fig. 11.** Residual-stress profiles in-depth of shot-peened AISI 420.

To compare the numerical results of this study with the experimental data of other papers, the relation between the Almen intensity and velocity can be used. Almen intensity in the finite intervals is linear in relation to velocity, which indicates that  $\sigma_{\text{surf}}^{\text{RS}}$  has very low dependency on Almen intensity. This result was consistent with the experimental results of ref. [34]

and their empirical formulas for AISI 4340 steel, and both steel behave the same. In ref. [34], it was concluded that the final effect of shot peening on  $\sigma_{\text{surf}}^{\text{RS}}$  is strongly dependent on the properties of the material itself. The direct relationship between stress and coverage percentage as the most important factor was seen in experiment data in ref. [35] too. It may be possible that different steels have similar behavior to the shot peening parameters that should be investigated in the future.

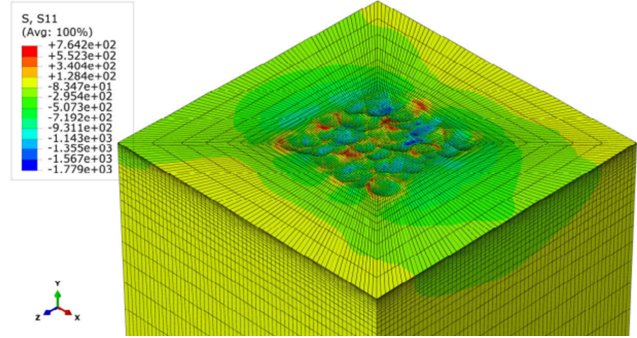


**Fig. 12.** Stress contour (S11) of shot peened surface.

It can be seen that  $\sigma_{\text{max}}^{\text{RS}}$  has a very low dependence on the shot velocity and Almen intensity. A similar behavior was found in the empirical equations of ref. [34] for  $\sigma_{\text{max}}^{\text{RS}}$ .

The  $\delta_{\text{max}}^{\text{RS}}$  had a linear relationship with velocity and consequently with Almen intensity. This equation was also in consistent with the empirical formula given in reference [34].

The  $\delta_{\text{max}}^{\text{RS}}$  had a linear relationship with velocity and hence Almen intensity. As in Eq. (18), this equation was consistent with the empirical formula in reference [34]. The relation of  $\delta_c^{\text{RS}}$  with different parameters was mentioned in references [36, 37].

Eq. (20) showed that Ra highly depended on the velocity of the shot and consequently was equal to that of Almen intensity. The results of this simulation were confirmed with the experimental results presented in reference [34]. It is seen here that Rc had a high dependence on velocity and less dependence on the other parameters.

## 6. Conclusions

The paper presented suitable and reliable methods to study and optimize the response variables (residual stress and surface roughness) simultaneously to determine the optimal parameters of the shot peening process. The main results were as follows:

1. The compressive residual stress and roughness parameter for different shot peening conditions could be predicted using the proposed model.
2. The surface residual stress is independent of shot

velocity and size, but depends on the coverage and sample thickness. The higher the coverage, the higher the compressive residual stress. The higher the thickness of the material, the less compressive stress is produced.

3. The maximum residual stress is independent of shot velocity and sample thickness, but depends on the coverage and the diameter of the shot. The higher the coverage, the higher the compressive residual stress. The higher the diameter of the shot, the higher the compressive residual stress.
4. The depth of maximum compressive stress is directly related to the velocity and diameter of the shot. The higher the velocity, the higher the depth of maximum compressive stress. The higher the diameter of the shot, the higher the depth of maximum compressive stress.
5. The depth of compressive stress depends on all of the studied parameters i.e. the diameter of the shot, shot velocity, coverage and sample thickness. However, the velocity and the diameter of the shot have the greatest impact. The higher the velocity, the higher the depth of compressive stress. The higher the diameter of the shot, the higher the depth of compressive stress.
6. Roughness has a linear relationship with shot velocity. The higher the velocity, the higher the roughness.
7. In other words, surface stress and maximum residual stress are independent of shot velocity, and other parameters are directly related to shot velocity.

## References

- [1] Society of Automotive Engineers, SAE Handbook: Automotive, Warrendale, PA, (1986).
- [2] R. Fathallah, H. Sidhom, C. Braham, L. Castex, Effect of surface properties on high cycle fatigue behaviour of shot peened ductile steel, *Mater. Sci. Technol.*, 19(8) (2003) 1050-1056.
- [3] A.M. Eleiche, M.M. Megahed, N.M. Abd-Allah, The shot-peening effect on the HCF behavior of high-strength martensitic steels, *J. Mater. Process. Technol.*, 113(1-3) (2001) 502-508.
- [4] D.A. Hills, R.B. Waterhouse, B. Noble, An analysis of shot peening, *J. Strain Anal. Eng. Des.*, 18(2) (1983) 95-100.
- [5] Y.F. Al-Obaid, Shot peening mechanics: experimental and theoretical analysis, *Mech. Mater.*, 19(2-3) (1995) 251-260.
- [6] S.T.S. Al-Hassani, Mechanical aspects of residual stress development in shot peening, *Shot Peening*, 583 (1981).
- [7] M. Obata, A. Sudo, Effect of shot peening on residual stress and stress corrosion cracking for cold worked austenitic stainless steel, in *Proceeding of the ICSP-5 Conference*, Oxford, UK, (1993) 258-264.
- [8] T. Dorr, M. Hilpert, P. Beckmerhagen, A. Kiefer, L. Wagner, Influence of shot peening on fatigue performance of high-strength aluminum-and magnesium alloys, *Proceedings of the ICSP-7 conference*, Warsaw, Poland, (1999) 153-160.
- [9] A.A. Ahmed, M. Mhaede, M. Basha, M. Wollmann, L. Wagner, The effect of shot peening parameters and hydroxyapatite coating on surface properties and corrosion behavior of medical grade AISI 316L stainless steel, *Surf. Coat. Technol.*, 280 (2015) 347-358.
- [10] S.B. Mahagaonkar, P.K. Brahmanekar, C.Y. Seemikeri, Effect of shot peening parameters on microhardness of AISI 1045 and 316L material: an analysis using design of experiment, *Int. J. Adv. Manuf. Technol.*, 38(5-6) (2008) 563-574.
- [11] Y.S. Nam, Y.I. Jeong, B.C. Shin, J.H. Byun, Enhancing surface layer properties of an aircraft aluminum alloy by shot peening using response surface methodology, *Mater. Des.*, 83 (2015) 566-576.
- [12] T. Hong, J.Y. Ooi, B. Shaw, A numerical simulation to relate the shot peening parameters to the induced residual stresses, *Eng. Fail. Anal.*, 15(8) (2008) 1097-1110.
- [13] S.A. Meguid, G. Shagal, J.C. Stranart, J. Daly, Three-dimensional dynamic finite element analysis of shot-peening induced residual stresses, *Finite Elem. Anal. Des.*, 31(3) (1999) 179-191.
- [14] M. Guagliano, Relating Almen intensity to residual stresses induced by shot peening: a numerical approach, *J. Mater. Process. Technol.*, 110(3) (2001) 277-286.
- [15] T. Kim, J.H. Lee, H. Lee, S.K. Cheong, An area-average approach to peening residual stress under multi-impacts using a three-dimensional symmetry-cell finite element model with plastic shots, *Mater. Des.*, 31(1) (2010) 50-59.
- [16] C. Wang, J. Hu, Z. Gu, Y. Xu, X. Wang, Simulation on residual stress of shot peening based on a symmetrical cell model, *Chin. J. Mech. Eng.*, 30(2) (2017) 344-351.

- [17] S.A. Meguid, G. Shagal, J.C. Stranart, 3D FE analysis of peening of strain-rate sensitive materials using multiple impingement model, *Int. J. Impact Eng.*, 27(2) (2002) 119-134.
- [18] A. Ghasemi, S.M. Hassani-Gangaraj, A.H. Mahmoudi, G.H. Farrahi, M. Guagliano, Shot peening coverage effect on residual stress profile by FE random impact analysis, *Surf. Eng.*, 32(11) (2016) 861-870.
- [19] H.Y. Miao, S. Larose, C. Perron, M. Lévesque, On the potential applications of a 3D random finite element model for the simulation of shot peening, *Adv. Eng. Software*, 40(10) (2009) 1023-1038.
- [20] A.H. Mahmoudi, A. Ghasemi, G.H. Farrahi, K. Sherafatnia, A comprehensive experimental and numerical study on redistribution of residual stresses by shot peening, *Mater. Des.*, 90 (2016) 478-487.
- [21] T. Kim, H. Lee, S. Jung, J.H. Lee, A 3D FE model with plastic shot for evaluation of equi-biaxial peening residual stress due to multi-impacts, *Surf. Coat. Technol.*, 206(13) (2012) 3125-3136.
- [22] S.M.H. Gangaraj, M. Guagliano, G.H. Farrahi, An approach to relate shot peening finite element simulation to the actual coverage, *Surf. Coat. Technol.*, 243 (2014) 39-45.
- [23] D. Hu, Y. Gao, F. Meng, J. Song, Y. Wang, M. Ren, R. Wang, A unifying approach in simulating the shot peening process using a 3D random representative volume finite element model, *Chin. J. Aeronaut.*, 30(4) (2017) 1592-1602.
- [24] M.E. Korkmaz, M. Günay, Finite element modelling of cutting forces and power consumption in turning of AISI 420 martensitic stainless steel, *Arab. J. Sci. Eng.*, 43(9) (2018) 4863-4870.
- [25] T. Kim, H. Lee, H.C. Hyun, S. Jung, Effects of rayleigh damping, friction and rate-dependency on 3D residual stress simulation of angled shot peening, *Mater. Des.*, 46 (2013) 26-37.
- [26] F. Yang, Y. Gao, Predicting the peen forming effectiveness of Ti-6Al-4V strips with different thicknesses using realistic finite element simulations, *J. Eng. Mater. Technol.*, 138(1) (2016) 011004.
- [27] D. Kirk, Theoretical principles of shot peening coverage, *Shot Peener*, 19(2) (2005) 24.
- [28] D.C. Montgomery, *Introduction Statistical Quality Control*, John Wiley & Sons Inc. Global Education, (2012).
- [29] B. Bhuvanaraghan, S.M. Srinivasan, B. Maffeo, Numerical simulation of Almen strip response due to random impacts with strain-rate effects, *Int. J. Mech. Sci.*, 53(6) (2011) 417-424.
- [30] A. Gariépy, H.Y. Miao, M. Lévesque, Simulation of the shot peening process with variable shot diameters and impacting velocities, *Adv. Eng. Software*, 114 (2017) 121-133.
- [31] L. Wagner, Mechanical surface treatments on titanium, aluminum and magnesium alloys, *Mater. Sci. Eng., A*, 263(2) (1999) 210-216.
- [32] ENISO, Geometrical Product Specifications (GPS)-Surface Texture: Profile Method—Terms, Definitions and Surface Texture Parameters, ISO 4287 (1997).
- [33] D.S. Moore, G.P. McCabe, B. Craig, *Introduction to the Practice of Statistics*, W.H. Freeman: New York, (1993).
- [34] V. Llana, F.J. Belzunce, Study of the effects produced by shot peening on the surface of quenched and tempered steels: roughness, residual stresses and work hardening, *Appl. Surf. Sci.*, 356 (2015) 475-485.
- [35] X. Wang, Z. Wang, G. Wu, J. Gan, Y. Yang, H. Huang, J. He, H. Zhong, Combining the finite element method and response surface methodology for optimization of shot peening parameters, *Int. J. Fatigue*, 129 (2019) 105231.
- [36] K.A. Soady, B.G. Mellor, G.D. West, G. Harrison, A. Morris, P.A.S. Reed, Evaluating surface deformation and near surface strain hardening resulting from shot peening a tempered martensitic steel and application to low cycle fatigue, *Int. J. Fatigue*, 54 (2013) 106-117.
- [37] S. Srilakshmi, D.V. Vidyasagar, S. Devaki Rani, The role of residual stresses with various shot peening parameters on 12% Cr blading steel for LP turbine applications, *Int. J. Mech. Eng. Robot.*, 1(1) (2013) 90-96.